

Mass spectrometric characterization of the Rosetta Spacecraft contamination with ROSINA.

A. Bieler^{a,b}, K. Altwegg^b, H. Balsiger^b, J.-J. Berthelier^c, U. Calmonte^b, M. Combi^a, J. De Keyser^d, B. Fiethe^e, S. A. Fuselier^f, S. Gasc^b, T. Gombosi^a, K. C. Hansen^a, M. Hässig^f, A. Korth^g, L. Le Roy^b, U. Mall^g, H. Rème^{h,i}, M. Rubin^b, T. Sémond^b, V. Tenishev^a, C.-Y Tzou^b, J. H. Waite^f, and P. Wurz^b

^aUniversity of Michigan CLaSP, 2455 Hayward Street, Ann Arbor 48104, United States

^bUniversity of Bern, Sidlerstrasse 5, 3012 Bern, Switzerland

^cLATMOS/IPSL-CNRS-UPMC-UVSQ, 4 Avenue de Neptune, F-94100 Saint-Maur, France

^dBelgian Institute for Space Aeronomy, BIRA-IASB, Ringlaan 3, B-1180 Brussels, Belgium

^eInstitute of Computer and Network Engineering (IDA), TU Braunschweig,

Hans-Sommer-Straße 66, D-38106 Braunschweig, Germany

^fSpace Science and Engineering Division, Southwest Research Institute, 6220 Culebra Road, San Antonio, Texas 78228, USA

^gMax-Planck-Institut für Sonnensystemforschung, Justus-von-Liebig-Weg 3, 37077 Göttingen, Germany

^hUniversité de Toulouse–UPS-OMP-IRAP, 31400 Toulouse, France

ⁱCNRS-IRAP, 9 avenue du Colonel Roche, BP 44346, F-31028 Toulouse Cedex 4, France

ABSTRACT

Mass spectrometers are valuable tools for the in situ characterization of gaseous exo- and atmospheres and have been operated at various bodies in space. Typical measurements derive the elemental composition, relative abundances, and isotopic ratios of the examined environment. To sample tenuous gas environments around comets, icy moons, and the exosphere of Mercury, efficient instrument designs with high sensitivity are mandatory while the contamination by the spacecraft and the sensor itself should be kept as low as possible. With the Rosetta Orbiter Spectrometer for Ion and Neutral Analysis (ROSINA), designed to characterize the coma of comet 67P/Churyumov-Gerasimenko, we were able to quantify the effects of spacecraft contamination on such measurements. By means of 3D computational modeling of a helium leak in the thruster pressurization tubing that was detected during the cruise phase we examine the physics involved leading to the measurements of contamination. 3 types of contamination can be distinguished: i) Compounds from the decomposition of the spacecraft material. ii) Contamination from thruster firing during maneuvers. iii) Adsorption and desorption of the sampled environment on and from the spacecraft. We show that even after more than ten years in space the effects of i) are still detectable by ROSINA and impose an important constraint on the lower limit of gas number densities one can examine by means of mass spectrometry. Effects from ii) act on much shorter time scales and can be avoided or minimized by proper mission planning and data analysis afterwards. iii) is the most difficult effect to quantify as it changes over time and finally carries the fingerprint of the sampled environment which makes prior calibration not possible.

Keywords: Contamination, Spacecraft, Rosetta, ROSINA, Mass spectrometry, Comets, 67P/Churyumov-Gerasimenko

Further author information: (Send correspondence to A.A.A.)

A.A.A.: E-mail: aaa@tbk2.edu, Telephone: 1 505 123 1234

B.B.A.: E-mail: bba@cmp.com, Telephone: +33 (0)1 98 76 54 32

1. INTRODUCTION

Advances in the development of mass spectrometers and technology in general leads to ever more powerful and sensitive instruments for planetary missions. Limitations on instrument performances that result from spacecraft contamination have been reported previously for remote sensing^{1,2} and in situ instruments.³ Organic compounds and H₂O ice deposit on optically sensitive surfaces such as mirrors and lenses of remote sensing instruments. Careful and long term heating of the affected elements can reduce or even eliminate contamination. For in situ instruments such as ROSINA the situation is different as the effects of spacecraft contamination are not only long term, but also manifest themselves on much shorter timescales. With ROSINA the currently most sensitive suite of mass spectrometers for space applications was launched in 2004 to rendez-vous with comet 67P/Churyumov-Gerasimenko (hereafter 67P) in 2014 and the spacecraft contamination had been characterized previously with ROSINA during the cruise phase en route to 67P.⁴ Heating of the mass spectrometer only prevents contamination from the instrument itself but is inefficient against the contamination from the rest of the spacecraft. Discrimination between molecules originating from the decomposing spacecraft and from the comet are not possible with ROSINA. This is especially harmful when low signals prevent a detailed analysis of the isotopic ratios that are potentially different from Earth.

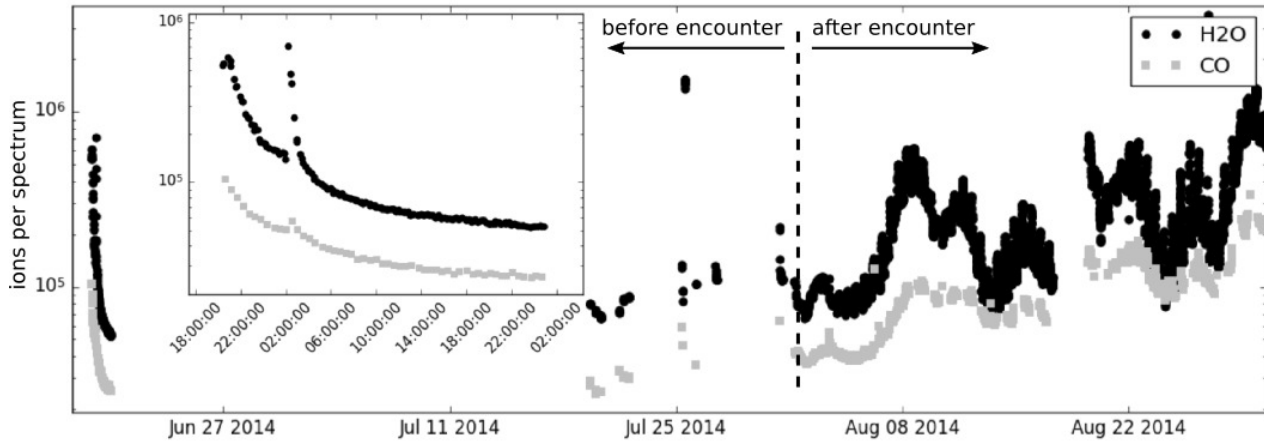


Figure 1. ROSINA-DFMS measurements for H₂O and CO for the rendezvous phase with 67P. The left hand side of the Figure shows the effect of a spacecraft maneuver for those two species. After this maneuver on 18 June 2014 it takes more than 24 hours for the contamination signal to fall off. In July 2014 DFMS was not operated continuously as the cometary signal was still too weak then. Starting from early August 2014 Rosetta was close enough to the comet to detect its neutral coma.

2. THE ROSINA INSTRUMENT SUITE

The ROSINA instrument suite on-board Rosetta consists of two mass spectrometers, RTOF (Reflectron Time Of Flight) and DFMS (Double Focusing Mass Spectrometer) and the pressure sensor COPS (COmet Pressure Sensor). RTOF and DFMS are designed to measure the relative abundances and isotopic ratios of neutrals and ions in the tenuous coma of 67P/Churyumov-Gerasimenko. COPS has two sensors, a nude gauge (NG) which measures the total number density of the neutrals at the spacecraft's location. Second, COPS has a ram gauge (RG) which is preferentially pointed towards the the comet nucleus (anti-parallel to the gas velocity vector) and measures the ram pressure of the outflowing gas in a small ante-chamber. When combining both gauges (NG and RG) one can deduce the outflow velocity of the gas. In this study we focus on data from DFMS and the COPS nude gauge only. The important difference is that COPS is not able to determine the composition of the coma, but only the total number density. COPS nude gauge measurements are accurate to 10% and evaluated with a resolution of one minute for the data presented in this study. DFMS has a resolving power of $m/\Delta m = 3000$ at the 1% peak level (at mass/charge 28 Da/e) which allows for the separation of CO and N₂. With a high dynamic range of 7+ decades and high sensitivity it is possible to measure very minor species in the coma of 67P with integration times of 20 s. As a scanning instrument in the Nier-Johnson configuration it takes about

30 minutes to accumulate a full mass spectrum ranging from 12 Da to 50 Da/e at the given integration time for a single measurement. This total accumulation time is on the same time scale as the contamination effects observed during spacecraft slewing as will be discussed in Section 6.

3. DATA REDUCTION AND TREATMENT

A typical set of DFMS measurements in high resolution mode is shown in Figure 5. The data from each panel in Figure 5 are the result of a 20 s integration and spans only over a narrow mass to charge (m/z) range around the integer values. DFMS has a position sensitive MCP (Micro Channel Plate) detector with two rows (row-A and row-B) of 512 bins along the dispersive axis of the instrument. Every peak is automatically identified and fitted with a Gaussian to compute the peak area. This area then corresponds to the total number of ions on the detector. It is important to note that cometary (and spacecraft) neutrals are ionized inside DFMS' ion source and hence impact the detector as ions. Row-A and row-B show different sensitivities and are evaluated independently. Finally the sum of the integrals of both rows are summed to get the total signal. In this study we will focus on data from DFMS neutral mode only. In this mode ambient positive ions are accelerated into the instrument by an additional potential of 200 Volts so that their energy is too high to pass through the analyzer section which has an energy acceptance of $dE/E \approx 1\%$. The Gaussian approximation introduces a systematic error of $< 10\%$ for all considered species as the real peak shape of the signal has on both sides wider tails than a pure Gaussian. If required, this extra peak broadening can be accounted for by adding a second Gaussian which is low in amplitude and broader than the first one. DFMS mass spectra are corrected for the detector degradation of the 512 individual bins of each row. Dedicated measurement modes were performed throughout the prime mission to characterize the individual bin degeneration. In those measurements the ion beam is moved across the detector to obtain a data set for the individual pixel calibration.

4. HELIUM LEAK AS TEST CASE

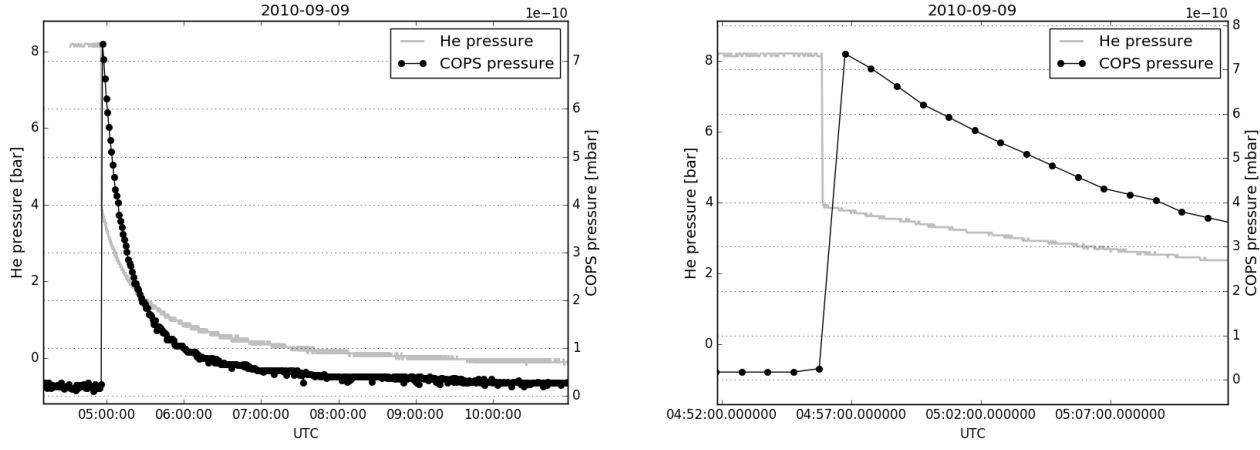


Figure 2. He and COPS ambient pressure during the valve pressurization test on 9 September 2009. **Left:** The full measurement set shows an instant reaction of COPS after the valve to a leaking section of the spacecraft pressurization tubing was opened. At the same time the He pressure decreases rapidly over the course of several hours. **Right:** A close up of the initial pressure change after the opening of the valve.

The Rosetta spacecraft has four 35 liter pressure tanks⁵ which are used to pressurize the hydrazine and the oxidizer chambers. The tubing connecting those tanks is divided into several segments. Each of these segments can be sealed individually by valves. During the cruise phase it was found that the pressure in one of the intermediate sections of this system was rapidly decreasing after being pressurized with helium. To determine whether this was a real gas leak or caused by a faulty pressure gauge it was decided to perform assisting measurements with ROSINA-COPS during one of these pressurization sequences. Figure 2 shows the result of

this test on two different time scales. The procedure was to inspect each segment individually by continuously opening a series of valves while monitoring the pressure. Indeed, after opening one of the valves ROSINA-COPS was able to measure a strong and rapid increase in total gas number density shortly after the questionable section of the piping was filled with He. In both panels of Figure 2 one can see the simultaneous pressure drop in the spacecraft piping and a fast increase in pressure measured by COPS. On the right panel of Figure 2 two separate stages of the pressure decay can be identified. The first one is due to the opening of the valve which allows He to expand into a bigger volume, causing an instant drop in pressure. Second, the now lower pressure level is not stable, but gradually falls off as He leaks out of the piping.

During this leak analysis campaign ROSINA-COPS was recording the ambient pressure once every minute. During this time the COPS signal peaked within one minute (which is the time-resolution of COPS) after opening the valve with a maximum He pressure of $7.5 \cdot 10^{-10}$ mbar. After several hours the COPS pressure returned to values similar to the initial state. One can clearly see the similar behavior between the COPS pressure measurements and the recorded He pressure from the spacecraft on the left hand side of Figure 2 as both see a decrease over several hours. However, what is also quite intriguing is the different decay factor of the exponential function. Either way, the detection of an actual leak was evident.

Scientifically more interesting than the confirmation of a leak in the tubing is the question on the gas kinetics involved for COPS being able to measure the escaping He. Due to the design and construction of the spacecraft we assume that there is no direct flow of He from inside the spacecraft (where the leak is) to COPS. The spacecraft body has a dedicated venting tube, located on the -z panel, hence on the opposite site of the COPS sensor at the underside of the spacecraft (see Figure 2). Numerical simulations using a Direct Simulation Monte Carlo (DSMC) method, with the Adaptive Mesh Particle Simulator (AMPS)^{6–8} code were performed in order to simulate the escaping He from the vent. For these simulations a (simplified) 3 dimensional model of the Rosetta spacecraft was created. Gas kinetics of millions of individual computational gas particles are computed in a segmented 3 dimensional simulation domain around the spacecraft. Taking into account realistic gas-surface interactions one can simulate the gas flow around the spacecraft. As soon as the gas pressure reaches equilibrium inside the spacecraft the loss rate through the venting tube is equal to the loss rate from the pressurized He tubing. This has been verified for different volume fractions of empty space inside the spacecraft to be filled with He and different transmissions through the venting hole. What, however, was different were the time constants, i.e. how quickly the outgassing through the vent increased versus the flooding of the leaking section with He. The relative low number densities of the outflowing He gas of $\leq 5 \cdot 10^{11} \text{ m}^{-3}$ make self-scattering a very inefficient process for re-directing He atoms to COPS and cannot explain the observations. More likely is diffuse scattering of He off spacecraft surfaces. Depending on the position of the high gain antenna a non zero gas flux at the COPS location is possible due to diffuse scattering. However, as our simulations show this contribution is at least one order of magnitude too low to explain the observed COPS measurements.

If a direct path for the He through the spacecraft to COPS can be excluded this means that other collisional sources must be present. The nature of this alternative transport mechanism is however still unknown. The neutral gas cloud surrounding the spacecraft with a pressure of $\sim 10^{-11}$ mbar does not provide sufficient cross section (mean free path in the order of 10^4 km) to account for the measured He signal at COPS. A potential source for scattering may be realized by a trapped cloud of ions surrounding the spacecraft. These ions can be created by photo-ionization or electron attachment of photo-electrons to water molecules. These ions are attracted or repelled by the spacecraft potential, which varies around -10 V and +20 V over time.⁹ However, at the time of the He leak test, way before the spacecraft arrived at the comet the spacecraft potential was mostly positive due to photoelectrons emitted from the surface of the spacecraft. This would repel a positively charged ion cloud and in turn trap negatively charged ions. If an ion cloud is to be responsible for the scattering of the He gas it will also affect the species outgassing from spacecraft decomposition. There was no evidence of a correlation between the spacecraft potential and the amount of measured fluorine, which is considered to be mostly due to spacecraft and instrument outgassing (see Section 5). Hence, the ion cloud approach does not seem reasonable. Further simulations are needed in order to establish the parameters of a potential background atmosphere which can explain the ROSINA-COPS observations. The quick reaction time of COPS to the leaking He indicates that a collisional process is necessary, rather than ionization mechanisms which would also make parts of the outflowing gas susceptible to the spacecraft potential and the solar wind. However, the rather long half life times (10^3 – 10^5 s) for photoionization of neutrals makes this unlikely.

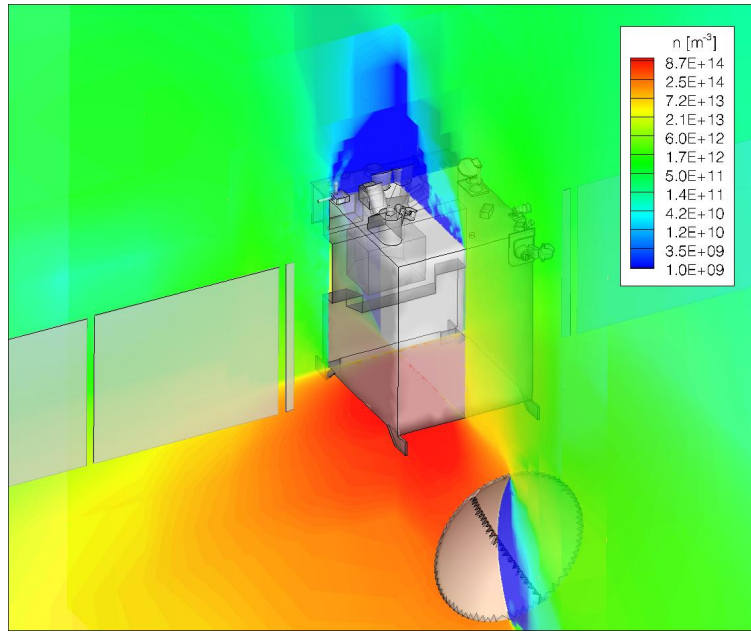


Figure 3. Gas number density distribution of He from the DSMC simulation when the He is released through the vent from the underside of the spacecraft. Number densities from reflections on spacecraft surfaces such as the backside of the high-gain antenna are about one order of magnitude too low to account for the measured signal by ROSINA-COPS.

5. TEMPORAL EVOLUTION OF THE CONTAMINATION

Fluorine has been identified early on during the cruise phase of Rosetta. It was detected with both ROSINA mass spectrometers, RTOF and DFMS⁴ and is attributed to lubricants. The fluorine peak is well resolved by DFMS and its continuous presence from laboratory calibrations throughout the cruise phase and during the prime mission make it a suitable test case to monitor the long term evolution of the spacecraft contamination during the prime mission. Contribution from the coma of 67P are expected to manifest themselves on time scales of \sim 12 hours akin to other cometary species. Figure 4 shows a time series of ROSINA-DFMS measurements from September 2014 to March 2015 at the $m/z=19$ line. Each data point in Figure 4 corresponds to the surface area of individual peaks as shown in Figure 5. The Fluorine peak is observed to be approximately constant during the whole inbound trajectory of 67P, from August 2014 to August 2015. The variations up to October 2014 may be attributed to the presence of cometary HF that fragments into H + F in the ion source of ROSINA-DFMS and hence contributes to the Fluorine peak. In contrast the other species at $m/z=19$ show much stronger variability over several orders of magnitude. Those variations are due to changing observation geometry of Rosetta (e.g. the radial distance from the nucleus changes), strong diurnal features and large scale heterogeneities within the coma of 67P.¹⁰ After perihelion however the fluorine peak gradually decreases over the course of 3 months until it is completely gone at around November 2015. An example post perihelion measurement from 26 January 2016 is shown in the right panel of Figure 5. We analyzed data up to June 2016 and the fluorine peak was not detected in this time frame. With ROSINA-RTOF the distinction between the four species on $m/z=19$ is harder to accomplish because of the lower resolving power and sensitivity compared to DFMS. It is currently unclear if the fluorine peak disappeared due to a change in the spacecraft environment during the outbound leg of 67P's trajectory or if the fluorine has finally escaped from the lubricants on Rosetta.

6. ADSORPTION AND DESORPTION DUE TO SPACECRAFT SLEWS

A time dependent component of spacecraft contamination is the adsorption and desorption of volatiles onto and from the spacecraft structure. Cold surfaces accumulate volatiles with high sublimation temperatures such as water (the dominating cometary volatile). These volatiles are quickly released once those surfaces warm up. This warming can be due to changing payload activities throughout the mission, where switching on a specific

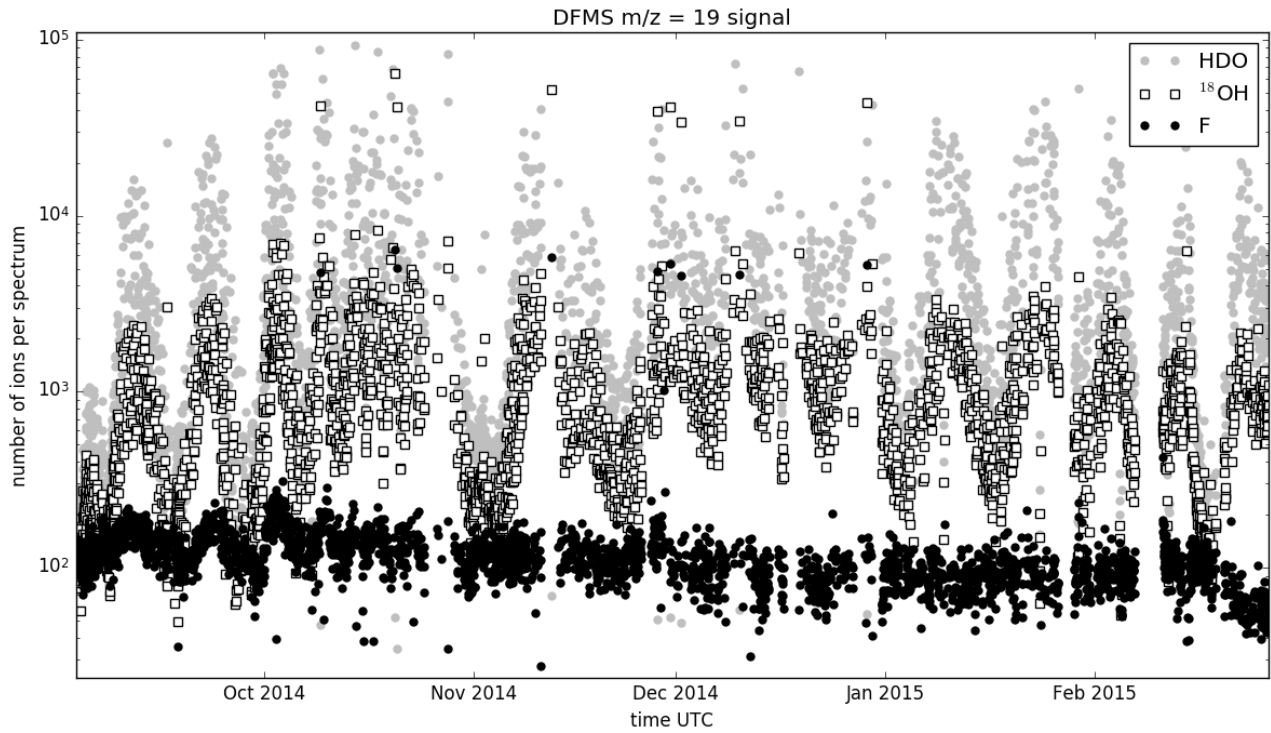


Figure 4. Evolution of the species with $m/q = 19$ Da/e as recorded by DFMS. In contrast to the water related signals of HDO and ^{18}OH which show large variations over time the Fluorine signal stays mostly constant over several months.

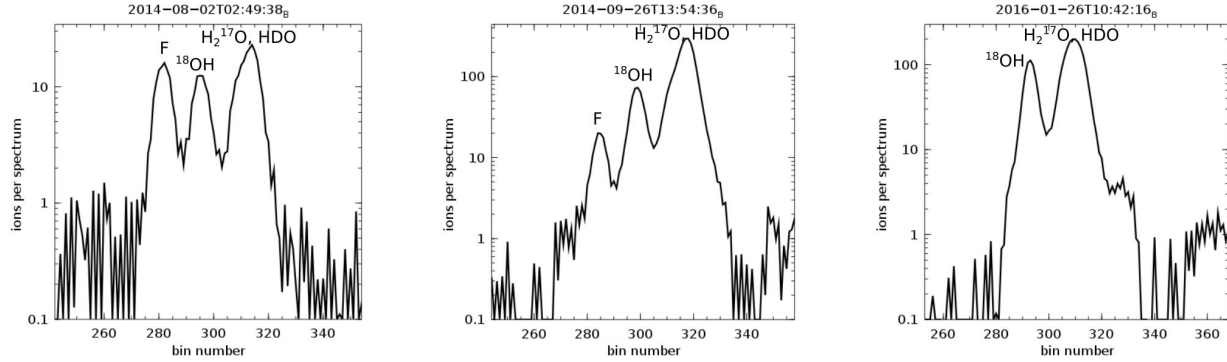


Figure 5. Evolution of the fluorine peak throughout the Rosetta mission. Four different species are identified in the $m/z=19$ range; the well separated F and ^{18}OH signals and in contrast the right most peak containing the two overlapping species of H_2^{17}O and HDO. **Left:** the fluorine peak is on the same order of magnitude as the other species around $m/z=19$. This measurement was taken before the close encounter with 67P and is the representative measurement of the spacecraft contamination. **Center:** during this measurement Rosetta was 10 km away from the comet nucleus center. The cometary species now dominate the spectrum with fluorine still on the same level as before the encounter with 67P. **Right:** measurement taken 5 months after perihelion, the fluorine peak has disappeared.

instrument warms up the local environment. The other possibility is that the illumination conditions on the spacecraft change, such that surface elements previously in the shadow receive sun-light, warm up and release volatiles. The released volatiles can be of spacecraft origin or from the atmosphere to be sampled. On Rosetta the pointing constraints of remote sensing instruments require active pointing and slewing over a significant amount of time. During these maneuvers, even though no thrusters are being fired and the attitude changes are realized through reaction wheels, the contamination from spacecraft outgassing is of the order of or even greater

than the cometary signature from 67P. Figure 6 shows an example of this effect. Open circles show the evolution of the Sun Angle in degrees. This angle is defined as the angle between the Sun pointing vector and the Rosetta +z axis. The +z axis on Rosetta coincides with the bore sight of the optical instruments and also the ROSINA mass spectrometers. All science instruments are located on the +z deck of the spacecraft, for Sun Angles > 90 degrees the entire instrument deck is in the shadow and for a Sun Angle of 180 degrees the Sun shines head on onto the -z deck, directly into the main thrusters of the spacecraft. In Figure 6 the open circles show the Sun Angle as a function of time for January 9th 2015. During this time a 'dust phase function observation' was performed, where the spacecraft's attitude changes over several hours in a circular motion. The instrument deck is initially pointed away from and finally towards the Sun to complete the circular motion. The Sun Angle varies between 180 deg and 20 deg during this maneuver.

6.1 Illuminated Instrument Deck

At around 16:00 UTC during the dust phase function observation the instrument deck becomes illuminated by the Sun (Sun Angle < 90 deg). During this phase the total pressure measured by COPS rapidly increases by more than a factor of four as indicated by the gray squares in Figure 6. The source of these pressure pulses can either be desorption of previously trapped volatiles on the spacecraft deck or heating up of dust grains collected on the +z deck that nominally points at the comet. This effect is observed for more than one hour after the Sun shines on the instrument deck aligned with the step-by-step changes of the Sun angle (plate on the right hand side). During this period the measured signal is completely dominated by the outgassing of the spacecraft and cometary measurements are not possible. In Figure 6 the typical cometary signal for 67P is seen as a roughly sine-shaped curve over the course of its rotation period of \sim 12 hours.^{11,12} We note that this spacecraft outgassing is very dynamic which makes it impossible to calibrate ahead of time or from previous maneuvers. This problem is most important for missions where short flybys are performed and stringent pointing requirements lead to quick attitude changes of the spacecraft with respect to the Sun.

For the last part of the great circle scan the Sun Angle is increasing. Both panels in Figure 6 show no contamination for this phase, even for very rapid and fast changes of the Sun angle. We attribute this to the fact that the illumination decreases and hence leads to lower energy input on the +z deck.

6.2 Illuminated Spacecraft Thrusters

A special case of increasing outgassing rates due to changing illumination conditions is observed for Sun Angles with magnitudes between 178 deg and 180 deg. For this configuration the Sun is almost in antiparallel direction to the spacecraft -z axis. A significant increase in number density is observed by ROSINA-COPS for this configuration. Black symbols on the left panel of Figure 6 indicate the corresponding data. The authors suggest this even stronger increase in number density is due to the Sun illuminating the spacecraft thrusters. Residual material from the fuel and oxidizer then sublimate quickly to produce the observed signal. Repeated observations of this phenomenon prove the effect is due to the changes in illumination and can not be attributed to changes in cometary activity. Hence, significant amounts of products from thruster firings may be 'discovered' by in situ mass spectrometers even after long periods from the last thruster operation. This puts some constraints on the pointing requirements for spacecraft missions to objects with heterogeneous atmospheres, such as comets.

7. CONTAMINATION COMPOSITION

The composition of the spacecraft contamination had previously been analyzed by Schläppi et al.⁴ for the cruise phase in 2010. A large number of organic molecules were identified from ROSINA-DFMS measurements and the largest contributions were seen from H₂O, CO, and CO₂. This picture is still true for July 2014, shortly before the close encounter of Rosetta with 67P. The composition before entering the coma of 67P is shown in the left panel of Figure 7. For the sake of simplicity these data have artificially been reduced to a unit mass resolution spectrum and is not corrected for the respective ionization cross section and sensitivity of the individual species. In this picture all peaks such as in e.g. Figure 5 are combined into a single bin at integer m/z=19. The full mass resolution of DFMS in our case is only needed for a few mass lines which will be discussed individually.

Rosetta went on a dayside excursion in September 2015 for several weeks. During this time the cometocentric distance was increased from a few 10s of km to 1500 km at the farthest point. The goal of this excursion was the

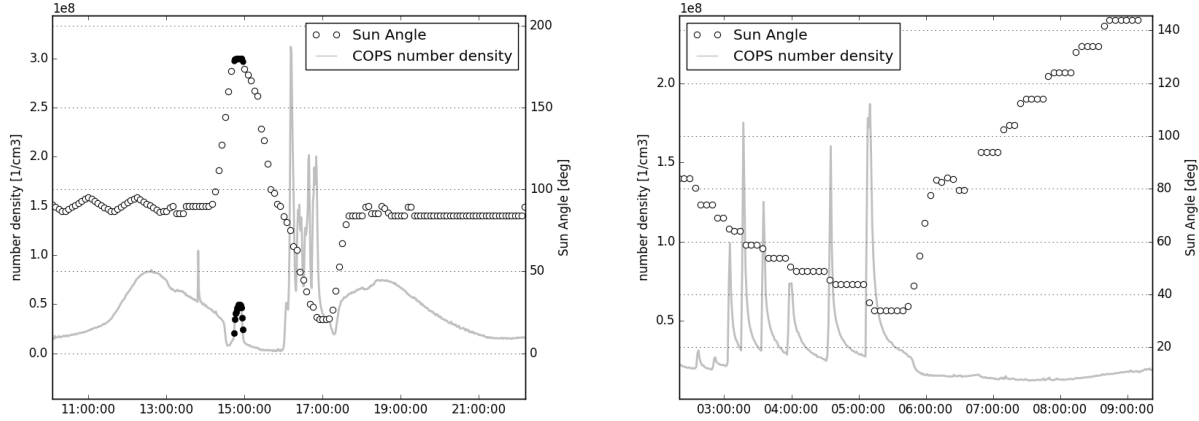


Figure 6. Two measurements with ROSINA-COPS during spacecraft slewing. Open circles show the evolution of the Sun Angle, defined as the angle between the $+z$ axis of the spacecraft and the Sun pointing vector. Gray lines show the neutral number density recorded by COPS. Filled black symbols indicate times where $178 \text{ deg} \leq \text{Sun Angle} \leq 180 \text{ deg}$ and are discussed in Section 6.2. **Left:** on 9 January 2015 Rosetta performed a circular scan for the remote sensing observations, for Sun Angle $\leq 90 \text{ deg}$ large signals from spacecraft contamination are recorded. **Right:** high outgassing rates are only observed while lowering the Sun Angle. Increasing the Sun angle does not influence the COPS measurements, even for Sun Angles $\leq 90 \text{ deg}$. We attribute this to a quick depletion of volatiles on the sunlit surfaces.

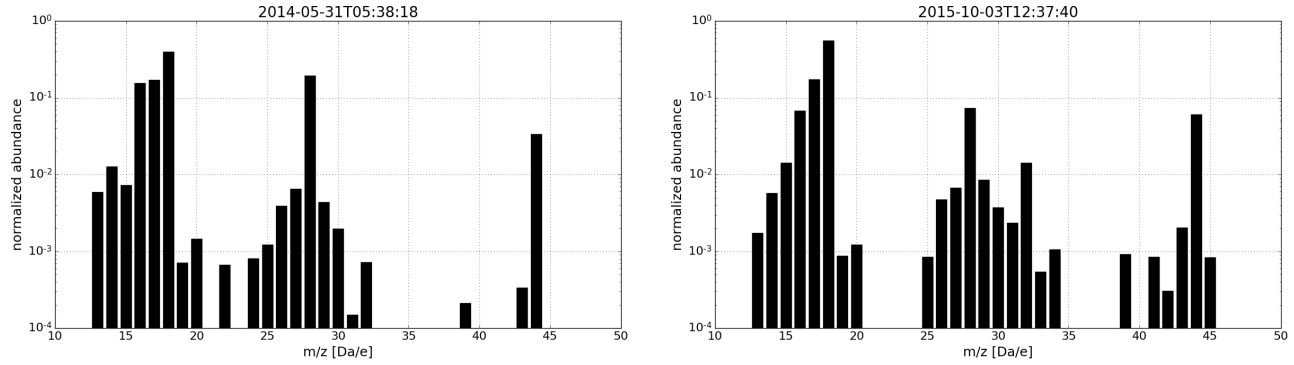


Figure 7. Comparison of the spacecraft composition measured by ROSINA-DFMS. **Left:** A typical background spectrum taken a few days before the close encounter with 67P/Churyumov-Gerasimenko. **Right:** Spacecraft contamination measurement after being exposed to the cometary coma for 14 months. The second measurement was taken at a distance of $> 1000 \text{ km}$ from the nucleus center.

characterization of the plasma environment close to perihelion. At this distance of the comet from the Sun the neutral coma of 67P beyond 1000 km is very tenuous. Hence, the dayside excursion can be used to perform a new set of background measurements at large cometocentric distances. The result of this background characterization campaign is shown in the right panel of Figure 7. The measured amount of H₂O is slightly higher than for the May 2014 data. Hence the coma still contributes to some extent to these measurements. Not surprisingly the background composition changed significantly since the last measurement of May 2014 and now resembles the coma composition of 67P. Mass lines 16 to 18 are now being dominated by the water group (H₂O, OH and O) with OH and O being mostly from fragmented H₂O. Before the close encounter the m/z=16 bin was relatively more abundant than can be explained with fragments of H₂O. In full resolution spectra it is clear that this additional signal is also due to OH and not from contributions of methane or NH₂. Also much more prominent is the m/z=32 mass line that gets contributions from fragments of sulfur bearing species and molecular oxygen, previously undetected in the background characterization.

8. CONCLUSIONS

Using 3D gas kinetic models we have shown that the simple picture of gas sublimation from the surface with diffuse scattering on spacecraft elements is not sufficient to explain scattering of volatiles of spacecraft origin around Rosetta. Neutral-ion collisions caused by a population of ions around the spacecraft can be excluded as mechanism as the measured contamination levels are independent of the spacecraft potential. It is however still unclear what other physical processes can cause the transport of volatiles around a spacecraft. Second, we examined the spacecraft contamination during spacecraft slews. We can show that accumulated material on cold surfaces or from collected dust grains instantly sublimates when illumination conditions on the spacecraft change. This effect is even more amplified for cases where the instrument deck is illuminated by the Sun. It is further shown that the depletion on sunlit surfaces happens on time scales of typically 10s of seconds and that after that further slewing does not lead to any more contamination. Finally it was observed that over time the composition of the contamination resembles the environment to be characterized by the measurements. Also going closer to the source, i.e. the comet in our case, improves the situation only marginally as the increased flux of volatiles and dust also lead to more trapping of gas on the cold surfaces and collection of dust. Without dedicated measurements to characterize the contamination over time its influence cannot be fully accounted for. Even for relatively stable contamination conditions the instrument's degradation (typically the MCPs of the detector) over time makes continuous characterization of the contamination levels necessary.

ACKNOWLEDGMENTS

Work at the University of Michigan was funded by NASA contract JPL-1266313. Work at the University of Bern was funded by the State of Bern, the Swiss National Science Foundation and the European Space Agency PRODEX Program. Work at Max-Planck-Institut für Sonnensystemforschung was funded by the Max-Planck Society and BMWI contract 50QP1302. Work at Southwest Research Institute was supported by subcontract 1496541 from the Jet Propulsion Laboratory. Work at BIRA-IASB was supported by the Belgian Science Policy Office via PRODEX/ROSINA PEA 90020. This work was carried out thanks to the support of the A*MIDEX project (no. ANR-11-IDEX-0001-02) funded by the ‘Investissements d’Avenir’ French Government programme, managed by the French National Research Agency (ANR). This work was supported by CNES grants at IRAP, LATMOS, LPC2E, UTINAM, CRPG, and by the European Research Council (grant no. 267255 to B.M.). Work by J.H.W. at Southwest Research Institute was funded by NASA JPL subcontract NAS703001TONMO710889. We acknowledge here the work of the whole ESA Rosetta team.

REFERENCES

- [1] Plucinsky, P. P., Schulz, N. S., Marshall, H. L., Grant, C. E., Chartas, G., Sanwal, D., Teter, M., Vikhlinin, A. A., Edgar, R. J., Wise, M. W., Allen, G. E., Virani, S. N., DePasquale, J. M., and Raley, M. T., “Flight spectral response of the ACIS instrument,” in [*X-Ray Gamma-Ray Telesc. Instruments Astron. Ed. by Joachim E. Truemper, Harvey D. Tananbaum. Proc. SPIE, Vol. 4851, pp. 89-100 (2003).*], **4851**, 89–100 (2003).
- [2] Bhaskaran, S., Mastrodemos, N., Riedel, J. E., and Synnott, S. P., “Optical navigation for the stardust wild 2 encounter,” in [*Eur. Sp. Agency, (Special Publ. ESA SP)*, (548), 455–460 (2004)].
- [3] Schläppi, B., Altwegg, K., Balsiger, H., Calmonte, U., Hässig, M., Hofer, L., Jäckel, A., Wurz, P., Berthelier, J., de Keyser, J., Fiethe, B., Fuselier, S., Mall, U., Rème, H., and Rubin, M., “Characterization of the gaseous spacecraft environment of Rosetta by ROSINA,” in [*3rd AIAA Atmos. Sp. Environ. Conf.*], (2011).
- [4] Schläppi, B., Altwegg, K., Balsiger, H., Hässig, M., Jäckel, A., Wurz, P., Fiethe, B., Rubin, M., Fuselier, S. A., Berthelier, J. J., De Keyser, J., Rème, H., and Mall, U., “Influence of spacecraft outgassing on the exploration of tenuous atmospheres with in situ mass spectrometry,” *J. Geophys. Res. Sp. Phys.* **115**(12), 1–14 (2010).
- [5] Glassmeier, K. H., Boehnhardt, H., Koschny, D., Kührt, E., and Richter, I., “The Rosetta mission: Flying towards the origin of the solar system,” *Space Sci. Rev.* **128**(1-4), 1–21 (2007).
- [6] Tenishev, V., Combi, M., and Davidsson, B., “A Global Kinetic Model for Cometary Comae: The Evolution of the Coma of the Rosetta Target Comet Churyumov-Gerasimenko throughout the Mission,” *Astrophys. J.* **685**(1), 659 (2008).

- [7] Tenishev, V., Combi, M. R., and Rubin, M., "Numerical simulation of dust in a cometary coma: Application to Comet 67P/Churyumov-Gerasimenko," *Astrophys. J.* **732**(2), 104 (2011).
- [8] Fougere, N., Combi, M. R., Rubin, M., and Tenishev, V., "Modeling the heterogeneous ice and gas coma of Comet 103P/Hartley 2," *Icarus* **225**(1), 688–702 (2013).
- [9] Odelstad, E., Eriksson, A. I., Edberg, N. J. T., Johansson, F., Vigren, E., André, M., Tzou, C.-Y., Carr, C., and Cupido, E., "Evolution of the plasma environment of comet 67P from spacecraft potential measurements by the Rosetta Langmuir probe instrument," *Geophys. Res. Lett.* **42**(23), 10,126–10,134 (2015).
- [10] Hässig, M., "Time variability and heterogeneity in the coma of 67P/Churyumov-Gerasimenko," *Science* **347**(6220), 1–5 (2015).
- [11] Bieler, A., Altwegg, K., Balsiger, H., Berthelier, J.-J., Calmonte, U., Combi, M., De Keyser, J., Fiethe, B., Fougere, N., Fuselier, S., Gasc, S., Gombosi, T., Hansen, K., Hässig, M., Huang, Z., Jäckel, A., Jia, X., Le Roy, L., Mall, U. A., Rème, H., Rubin, M., Tenishev, V., Tóth, G., Tzou, C.-Y., and Wurz, P., "Comparison of 3D kinetic and hydrodynamic models to ROSINA-COPS measurements of the neutral coma of 67P/Churyumov-Gerasimenko," *Astron. Astrophys.* **583**(November 2015), A7 (2015).
- [12] Mottola, S., Lowry, S., Snodgrass, C., Lamy, P. L., Toth, I., Sierks, H., Angrilli, F., Barbieri, C., Barucci, M. a., Cremonese, G., Davidsson, B., Cecco, M. D., Debei, S., Fornasier, S., Fulle, M., Groussin, O., Hviid, S. F., Ip, W., Jorda, L., Keller, H. U., Knollenberg, J., Koschny, D., Kramm, R., Lara, L., Lazzarin, M., Moreno, J. J. L., Marzari, F., Michalik, H., Naletto, G., Rickman, H., Rodrigo, R., Sabau, L., Thomas, N., Agarwal, J., Bertini, I., Ferri, F., Magrin, S., Oklay, N., Tubiana, C., Rožek, a., A'Hearn, M. F., Bertaux, J.-L., Da Deppo, V., De Cecco, M., Gutiérrez, P., Kührt, E., Küppers, M., Lopez Moreno, J. J., Wenzel, K.-P., Güttler, C., and Vincent, J.-B., "The rotation state of 67P/Churyumov-Gerasimenko from approach observations with the OSIRIS cameras on Rosetta," *Astron. Astrophys.* **569**, L2 (2014).